RSC Advances

COMMUNICATION

View Article Online
View Journal | View Issue

Cite this: *RSC Adv.*, 2016, **6**, 75227

Received 2nd June 2016
Accepted 1st August 2016

DOI: 10.1039/c6ra14352k

www.rsc.org/advances

A comparative study between heterogeneous stannous chloride loaded silica nanoparticles and a homogeneous stannous chloride catalyst in the synthesis of 5-substituted 1*H*-tetrazole†

Arvind Kumar,[a] Satyanand Kumar,[a] Yugal Khajuria[b] and Satish Kumar Awasthi*[a]

Heterogeneous $SnCl_2$–nano-SiO_2 efficiently catalyzed 5-substituted 1*H*-tetrazole synthesis with excellent yield. The catalyst was characterized by using FT-IR, TGA, TEM, and EDX. It is widely applicable on aliphatic, aromatic, heteroaromatic and sterically hindered nitriles with five time recyclability. Being simple and an economically viable approach for the synthesis of $SnCl_2$–nano-SiO_2 are additional advantages.

Tetrazoles are nitrogen rich heterocyclic compounds having a wide range of applications in the area of medicinal chemistry,[1–8] agriculture,[9] coordination chemistry[10] and material chemistry.[11] They are stable against a wide pH range, and various oxidizing and reducing agents.[12]

Initially, tetrazoles were synthesized by the reaction of hydrogen cyanide and anhydrous hydrazoic acid under pressure. These reagents are extremely toxic, water sensitive and low boiling liquids (HN_3, ~37 °C).[13] Later, Finnegan *et al.*[14] reported the improved procedure for synthesis of 5-substituted tetrazoles by (3 + 2) cycloaddition using inorganic azide in place of toxic hydrazoic acid. Subsequently, Sharpless *et al.*[15] pioneered tetrazole synthesis using Zn^{2+} salt as a Lewis acid catalyst. More recently, various homogeneous and heterogeneous catalysts such as Py HCl,[16] $Yb(OTf)_3 \cdot xH_2O$,[17] $(NH_4)_2Ce(NO_3)_6$,[18] Zn/Al hydrotalcite,[19] CoY zeolite,[20] Cu–Zn alloy nanopowder,[21] CAN-HY zeolite,[22] Au NPs,[23] PtNPs@Ac,[24] $FeCl_3$–SiO_2,[25] $NaHCO_3$-$\cdot SiO_2$,[26] $SiO_2 \cdot H_2SO_4$,[27] $Ln(OTf)_3 \cdot SiO_2$,[28] *etc.* were used in tetrazole synthesis. However, these catalysts suffer one or more drawbacks such as cost of catalysts, non-recyclability, water sensitivity, tedious synthesis procedure, longer reaction time, higher reaction temperature, lower yield, and excess use of catalyst, *etc.* Moreover, most of the above mentioned catalysts were not widely applicable on all type of nitriles (aliphatic, aromatic, heteroaromatic, sterically hindered aromatic nitrile) with excellent efficiency. Thus, these drawbacks encouraged us to design an efficient catalyst which is cost effective, recyclable, and equally useful to aliphatic, aromatic, heteroaromatic and sterically hindered aromatic nitriles with various electron withdrawing or electron donating functionalities.

The literature survey reveals that tin salts show high Lewis acidity as compared to other transition metals and the order is $Sn^{2+} \gg Zn^{2+} > Pb^{2+} \approx Hg^{2+}$.[29] To keep it in mind that Sn^{2+} salt has higher Lewis acidity in comparison to other metal salts, we have selected $SnCl_2$ as homogeneous catalyst. Further, in the last few years, some metal salts *viz.* Fe, Sb *etc.* immobilized on silica support have received considerable attention in tetrazole synthesis,[30–36] but these were suffer with several drawback such as longer reaction time, lesser recyclability, higher loading of catalyst *etc.* To improve upon the catalyst efficiency, catalyst loading, applicability and recyclability of the catalyst, we choose silica nanoparticles as it has high surface area, large pore volume, and recyclable tendency; hence, it may be useful as support for immobilization of Sn^{2+} salts. We immobilized $SnCl_2$ by reaction of hydroxyl groups on silica (Scheme 1), thus homogeneous $SnCl_2$ catalyst converted into heterogeneous catalyst with improved features for the synthesis of 5-substituted 1*H*-tetrazole synthesis.

Our research group has been working on diversified area such, catalysis, asymmetric synthesis, and design, synthesis of malaria inhibitor.

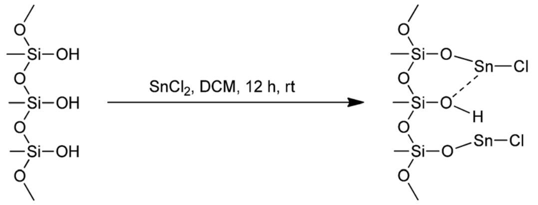

Scheme 1 Probable structure of covalently anchored $SnCl_2$–nano-SiO_2.

---

[a] *Chemical Biology Laboratory, Department of Chemistry, University of Delhi, Delhi-110007, India. E-mail: satishpna@gmail.com; skawasthi@chemistry.du.ac.in*

[b] *School of Physics, Shri Mata Vishno Devi University, Katra, Jammu and Kashmir, India*

† Electronic supplementary information (ESI) available: X-Ray analysis, NMR and IR data are given. CCDC 999827. For ESI and crystallographic data in CIF or other electronic format see DOI: 10.1039/c6ra14352k

Herein, we report an efficient, recyclable, widely applicable and easy to prepare $SnCl_2$–nano-SiO_2 as heterogeneous catalyst for 5-substituted 1*H*-tetrazole synthesis and compared its efficiency with homogeneous $SnCl_2$ catalyst.

Preparation of $SnCl_2$–nano-SiO_2

$SnCl_2$–nano-SiO_2 was synthesized using procedure reported in literature.[37] Briefly, 2.0 g of silica nanoparticles of 25 nm size and (1.2 g, 6.32 mmol) of $SnCl_2$ were suspended in 20 mL of dichloromethane and the resulting suspension was stirred for overnight. After this period, the resulting suspension was filtered and the catalyst was washed with CH_2Cl_2 and the solid powder was dried in high vacuum for 5 hours at 100 °C, until a free flow powder of $SnCl_2$–nano-SiO_2 was achieved. $SnCl_2$–nano-SiO_2 was characterized by FT-IR, XRD, TEM, EDX and TGA analysis. The proposed structure of $SnCl_2$–nano-SiO_2 catalyst in which $SnCl_2$ may have reacted with the surface hydroxyl group of silica nanoparticles is shown in Scheme 1.

FT-IR analysis of $SnCl_2$–nano-SiO_2

To identify the structure of $SnCl_2$–nano-SiO_2, we studied IR spectra of $SnCl_2$–nano-SiO_2 (Fig. 1). The FT-IR spectrum displays characteristic peaks at 1102 and 806 cm^{-1} corresponding to symmetrical and asymmetrical vibrations of Si–O–Si, respectively while the Sn–Cl and Si–OH resonances were observed in 1564 and 3428 cm^{-1} respectively.[37,38] The successful covalent linking of the $SnCl_2$ on the surface of SiO_2 was confirmed by the appearance of a new band at 541 cm^{-1}, which originates from the absorption of O–Sn (Fig. 1).[39]

Thermogravimetric analysis (TGA) of $SnCl_2$–nano-SiO_2

The TGA curves are plotted in the temperature range of 25–800 °C with heating at the rate of 5 °C min^{-1} under nitrogen atmosphere. TGA plots of SiO_2, fresh $SnCl_2$–nano-SiO_2 and recycled $SnCl_2$–nano-SiO_2 showed initial weight loss up to 100 °C, which is calculated as 3.43%, 7.27% and 6.85% respectively. This weight loss can be generally attributed due to the loss of surface physisorbed water. Further, the TGA curves of SiO_2, fresh $SnCl_2$–nano-SiO_2 and 5 times recycled $SnCl_2$–nano-SiO_2 showed again weight loss in temperature range of 100–800 °C, which is calculated as 3.36%, 15.77% and 14.53% respectively. Fresh $SnCl_2$–nano-SiO_2 may showed this weight loss due to physisorbed and chemisorbed $SnCl_2$ from the surface of the silica nanoparticles, while 5 time cycle used $SnCl_2$–nano-SiO_2 may showed this weight loss only due to chemisorbed $SnCl_2$. SiO_2 showed weight loss in 100–800 °C temperature range due to condense of water molecules between

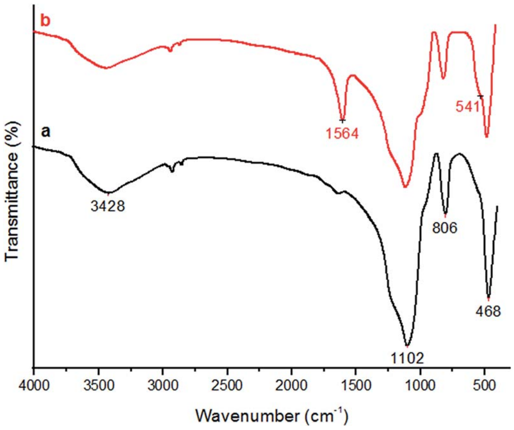

Fig. 1 FT-IR spectra of (a) SiO_2 and (b) $SnCl_2$–nano-SiO_2.

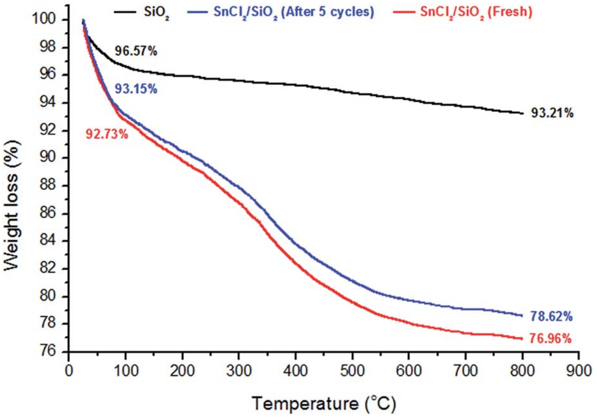

Fig. 2 TGA plots of SiO_2, $SnCl_2/SiO_2$ (fresh) and $SnCl_2/SiO_2$ (after 5 cycles).

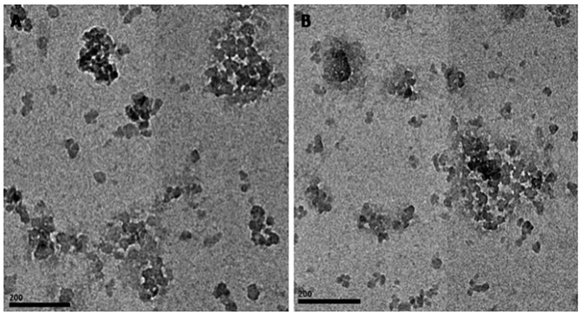

Fig. 3 TEM images of $SnCl_2$–nano-SiO_2 ((A) is before reaction and (B) is after reaction).

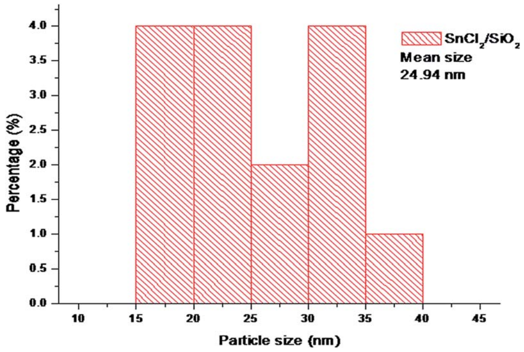

Fig. 4 Particle size of $SnCl_2$–nano-SiO_2.

hydroxyl groups at the surface of silica nanoparticles, as a result oxo bridges (Si–O–Si) are formed. The comparison of weight loss of SiO_2 and fresh $SnCl_2$–nano-SiO_2 revealed that 12.41% $SnCl_2$ is loaded on silica surface in fresh $SnCl_2$–nano-SiO_2 catalyst, while the comparison of weight loss of SiO_2 and 5 times recycled $SnCl_2$–nano-SiO_2 revealed that 11.17% $SnCl_2$ is loaded on silica surface in recycled $SnCl_2$–nano-SiO_2 catalyst. Thus, there is a marginal loss of activity in 5 times recycled $SnCl_2$–nano-SiO_2 as compared to fresh $SnCl_2$–nano-SiO_2 catalyst (Fig. 2).

High resolution TEM and EDX analysis of $SnCl_2$–nano-SiO_2

The size of $SnCl_2$–nano-SiO_2 catalyst was found to be approximately 25 nm as determined by the TEM images (Fig. 3). Size was calculated by image j software (Fig. 4). The Fig. 5 is about energy dispersive X-ray analysis of $SnCl_2$–nano-SiO_2 catalyst.

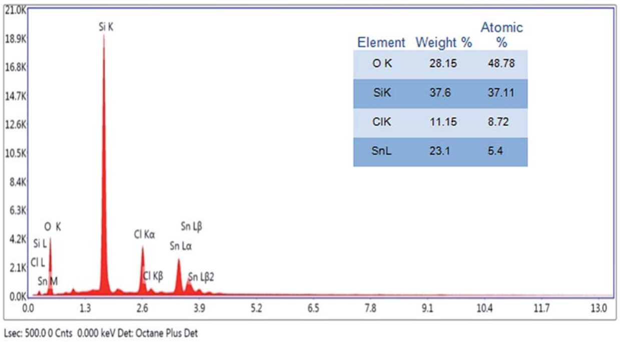

Fig. 5 The EDX spectrum of $SnCl_2$–nano-SiO_2.

Table 1 Effect of tin catalysts in synthesis of tetrazole **1b**

Entry	Catalyst[a,b]	Time (h)	Yield (%)
1	Sn[a]	8	60
2	$SnCl_2$[a]	6	90
3	$SnCl_2$–SiO_2[b]	4	92
4	$SnCl_4$[a]	6	85
5	Me_2SnCl_2[a]	6	82
6	SnI_4[a]	6	86
7	SiO_2[a]	6	12

[a] 10 mmol% of catalyst at 120 °C. [b] 5 mmol% of catalyst at 100 °C.

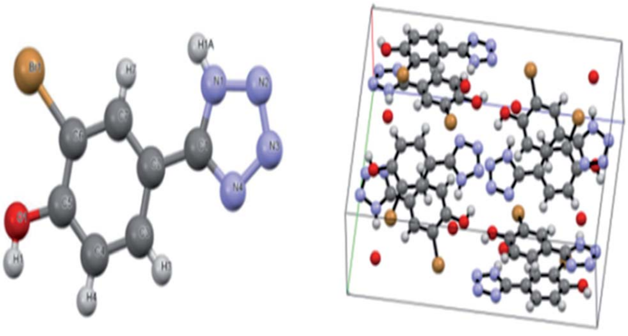

Fig. 6 X-Ray analyzed unit cell packing of compound **6b**.

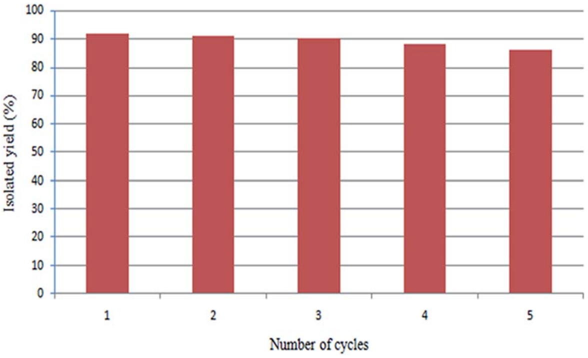

Fig. 7 Recyclability test.

Table 2 Effect of solvents in the synthesis of tetrazole **1b** by using $SnCl_2$[a] (C1) and $SnCl_2$–SiO_2[b] (C2) catalyst

Entry	Solvent	Temp (°C) (C1/C2)	Time (h) (C1/C2)	Yield (%) (C1/C2)
1	H_2O	100/100	12/12	0/0
2	EtOH	78/78	24/24	25/27
3	DMF	120/100	6/4	90/92
4	DMSO	120/100	12/12	68/72
5	NMP	100/100	12/12	65/68
6	Toluene	110/100	24/24	35/36
7	THF	66/66	24/24	30/32
8	CH_3CN	80/80	12/12	0/0
9	DCM	39/39	12/12	0/0
10	Acetone	56/56	12/12	0/0
11	1,4-Dioxane	100/100	12/12	0/0

[a] 10 mmol% of $SnCl_2$. [b] 5 mmol% $SnCl_2$–SiO_2 catalyst with 1 mmol of nitrile.

The EDX spectrum gives an idea of elemental composition of constituent elements like O, Si, Cl and Sn. Analysis confirms the presence of O, Si, Sn, and Cl elements, in the ratio of 48.78, 37.11, 8.72 and 5.4 atomic%. The *Y*-axis shows the counts (number of X-rays received and processed by the detector) and the *X*-axis shows the energy level of those counts.

Table 3 Effect of temperature and catalyst loading in the synthesis of tetrazoles **1b** in DMF

Entry	Catalyst (mmol%)	Temp (°C)	Time (h)	Yield[a] (%)
1	$SnCl_2$ (5)	100	6	66
2	$SnCl_2$ (5)	100	12	73
3	$SnCl_2$ (5)	120	6	78
4	$SnCl_2$ (5)	120	12	82
5	$SnCl_2$ (10)	100	12	83
6	$SnCl_2$ (10)	120	12	90
7	$SnCl_2$ (10)	120	6	90
8	$SnCl_2$ (15)	120	6	92
9	$SnCl_2$–SiO_2 (5)	100	4	92
10	$SnCl_2$–SiO_2 (5)	120	4	92
11	$SnCl_2$–SiO_2 (5)	120	6	92
12	$SnCl_2$–SiO_2 (10)	100	4	93
13	$SnCl_2$–SiO_2 (10)	120	4	93

[a] Isolated yield.

Table 4 Synthesis of 5-substituted 1*H*-tetrazoles

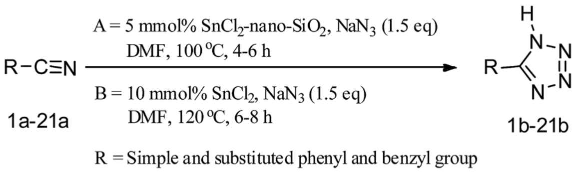

			Time (h)	Yield[c] (%)
Entry	Substrate[a]	Product	$SnCl_2$/$SnCl_2$–SiO_2	$SnCl_2$/$SnCl_2$–SiO_2
1	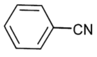	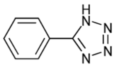	6/4	90/92
2	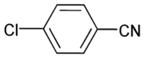	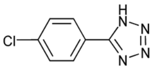	6/4	92/95
3	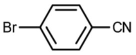	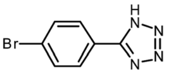	6/4	91/94
4	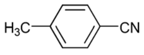	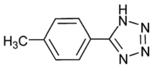	6/4	87/90
5	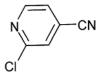	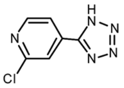	6/4	94/97
6	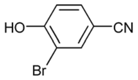	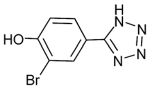	6/4	86/89
7	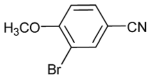	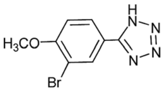	6/4	88/90
8	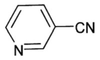	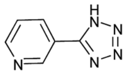	6/4	91/94
9	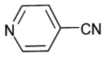	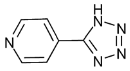	6/4	93/98
10	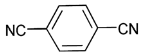	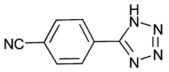	6/4	92/97
11	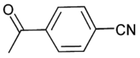	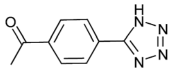	6/4	91/95
12	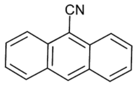	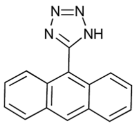	6/4	92/96
13	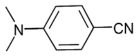	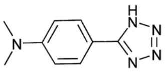	6/4	86/89
14	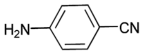	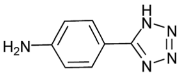	6/4	82/86
15	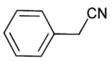	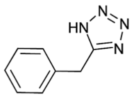	8/6	80/84

Table 4 (*Contd.*)

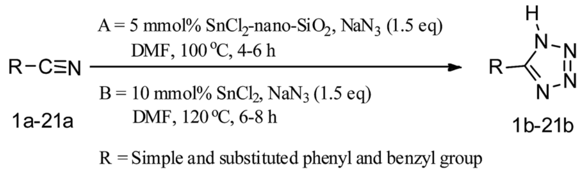

Entry	Substrate[a]	Product	Time (h)	Yield[c] (%)
			$SnCl_2/SnCl_2–SiO_2$	$SnCl_2/SnCl_2–SiO_2$
16	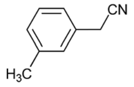	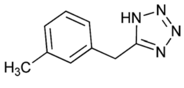	8/6	78/82
17	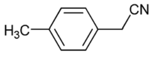	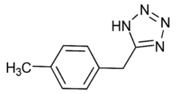	8/6	80/85
18	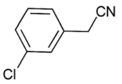	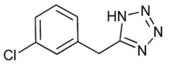	8/6	82/86
19	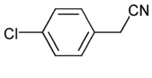	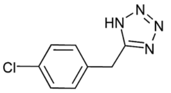	8/6	84/88
20	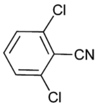	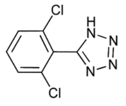	6/4	82/88
21[b]	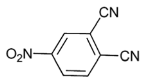	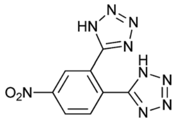	8/6	90/93

[a] The reaction of nitriles with NaN_3 (1.5 equiv.) was conducted in DMF in the presence of 10 mmol% of $SnCl_2$ at 120 °C and in presence of 5 mmol% of $SnCl_2$–nano-SiO_2 at 100 °C. [b] The reaction of nitrile with NaN_3 (3 equiv.) was conducted in DMF in the presence of 20 mmol% of $SnCl_2$ at 120 °C and in presence of 10 mmol% of $SnCl_2$–nano-SiO_2 at 100 °C. [c] Isolated yield (%).

We know that the selection of the catalyst is of utmost important to achieve good yield of a reaction. Therefore, initially we compared the catalytic activity among all *viz.* Sn(0), $SnCl_2$, $SnCl_2$–nano-SiO_2, $SnCl_4$, SnI_4 and Me_2SnCl_2 in the synthesis of tetrazole **1b**. Sn(0) gave poor yield (60%, Table 1, entry 1). $SnCl_2$–nano-SiO_2 catalyst showed highest catalytic activity followed by $SnCl_2$ in the synthesis of tetrazole **1b** (Table 1, entry 2 and 3). Catalysts $SnCl_4$, Me_2SnCl_2 and SnI_4 also gave good yield in the range of 82–86% (Table 1, entry 4–6). However, handling of $SnCl_4$ is difficult due to its highly volatile nature, while SnI_4 and Me_2SnCl_2 are very expensive, hence omitted from our present study. Silica showed very poor catalytic activity (12% yield) in tetrazole synthesis (Table 1, entry 7). Since silica showed poor catalytic activity, we exploited this property and immobilized $SnCl_2$ in order to get synergetic effect of $SnCl_2$ with SiO_2 due to the multiple Lewis acid catalytic centers. Moreover, by immobilizing $SnCl_2$ on SiO_2, the resultant catalyst shows better catalytic activity in compare to $SnCl_2$. Thus, we concentrated our efforts in the comparative study of tetrazole synthesis using homogeneous $SnCl_2$ and heterogeneous $SnCl_2$–nano-SiO_2 catalysts.

$SnCl_2$–nano-$SnCl_2$ catalyst was easily synthesized in cost effective manner which is recyclable and reusable catalyst. Recycling of the catalyst is an important factor in catalyst design which reduces the overall cost of catalyst. We tested this feature in case of $SnCl_2$–nano-SiO_2 in five subsequent cycles and showed minimum decrease in the isolated yields, hence minimum loss of catalytic efficiency (Fig. 7).

We optimized reaction solvent and DMF was found to be the best solvent for tetrazole synthesis (Table 2, entry 4), whereas dimethylsulfoxide and *N*-methylpyrrolidone provided moderate yields (Table 2, entries 4 and 5). After solvent optimization conditions, we investigated the effects of temperature and catalyst loading on the reaction yields and results are summarized in Table 3. We have found that 5 mmol% of $SnCl_2$–nano-SiO_2 at 100 °C or 10 mmol% of $SnCl_2$ at 120 °C gives better yields. Further increase in the catalyst loading has insignificant effect on yield (Table 3, entries 8 and 9).

We performed reaction by using $SnCl_2$–nano-SiO_2 (5 mmol%) at 100 °C for 4 h to get 92% yield (Table 3, entry 10). Further increase in catalyst loading and reaction temperature or reaction time did not increase the yield (Table 3 entries 11–14). Thus, 5 mmol% catalysts loading at 100 °C for 4 h reaction time is the optimal condition for $SnCl_2$–nano-SiO_2 catalyst while 10 mmol% catalysts loading at 120 °C for 6 h is the optimal condition for $SnCl_2$ catalyst. To authenticate the methodology, various aromatic and aliphatic nitriles were treated with sodium azide under optimized conditions using both catalysts (Table 4). The presence of heteroatom in the ring increases the reactivity of heteroaromatic nitriles (Table 4, entries 5, 8 & 9). Electron withdrawing group also increases the reactivity of aromatic nitriles so that electron withdrawing group with aromatic nitrile (Table 4, entries 2, 3, 10, 11 & 21) gave better yield than electron donating group with aromatic nitriles (Table 4, entries 4, 6, 7, 13 & 14). Aromatic nitriles gave slightly better yields of corresponding tetrazoles (Table 4, entries 1–14), as compared to aliphatic nitriles (Table 4, entries 15–19). This approach is also useful for the synthesis of heteroaromatic tetrazoles (Table 4, entries 5–9) and sterically hindered tetrazoles (Table 4, entries 20 and 21). To authenticate this methodology, we report herein crystal data of compound **6b** (Fig. 6).

Plausible mechanism

It is proposed that the lone-pair electrons of nitrogen in nitrile coordinate with tin(II) due to its Lewis acid behaviour.[40] As a result of coordination, it activates nitrile carbon for the nucleophilic attack by azide ion which forms intermediate [A], which undergoes rearrangement *via* (3 + 2) cycloaddition to produce [B]. The intermediate [B] subsequently converts to [C], with regeneration of $SnCl_2$, which on protonation with HCl gives tetrazole. The overall mechanism is depicted in Scheme 2.

Computational details

We did computational analysis to optimize geometry, structural parameters, HOMO–LUMO orbitals and vibrational bands of compound **6b** using DFT with 6-311G basis sets using Gaussian 09 program and found that calculated data was in good agreement with the experimental data (see 5–7 pages of ESI†).

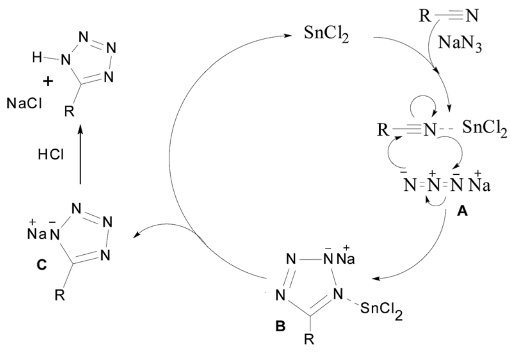

Scheme 2 Plausible mechanism for tetrazole synthesis.

Conclusions

In the present study, $SnCl_2$ and $SnCl_2$–nano-SiO_2 have been used for the synthesis of 5-substituted 1*H*-tetrazoles. Among these two catalysts, $SnCl_2$ and $SnCl_2$–nano-SiO_2 catalyst, later was most efficient in converting nitrile into tetrazole with high yield. Lesser reaction time, temperature, and lower loading of catalyst are additional advantages. Moreover, aromatic nitriles having electron withdrawing group are more reactive than having electron donating group. In addition, aromatic nitriles are more reactive than aliphatic nitrile toward tetrazole synthesis. This approach also works very well in conversion of sterically hindered nitriles to their respective tetrazoles.

Acknowledgements

AK and SK are thankful to UGC, New Delhi, India for Senior Research Fellowship and to USIC for analysis of our data. SKA is thankful to DU-DST Purse Grant & University of Delhi, Delhi-110007 for financial support.

Notes and references

1 R. J. Herr, *Bioorg. Med. Chem.*, 2002, **10**, 3379.
2 J. Roh, K. Vavrova and A. Hrabalek, *Eur. J. Org. Chem.*, 2012, 6101.
3 A. D. Sarro, D. Ammendola, M. Zappala, S. Grasso and G. B. D. Sarro, *Antimicrob. Agents Chemother.*, 1995, **39**, 232.
4 T. Mavromoustakos, A. Kolocouris, M. Zervou, P. Roumelioti, J. Matsoukas and R. Weisemann, *J. Med. Chem.*, 1999, **42**, 1714.
5 A. D. Abell and G. J. Foulds, *J. Chem. Soc., Perkin Trans. 1*, 1997, 2475.
6 Y. Tamura, F. Watanabe, T. Nakatani, K. Yasui, M. Fuji, T. Komurasaki, H. Tsuzuki, R. Maekawa, T. Yoshioka, K. Kawada, K. Sugita and M. Ohtani, *J. Med. Chem.*, 1998, **41**, 640.
7 R. E. Ford, P. Knowles, E. Lunt, S. M. Marshal, A. J. Penrose, C. A. Ramsden, A. J. H. Summers, J. L. Walker and D. E. Wrigth, *J. Med. Chem.*, 1986, **29**, 538.
8 E. A. Hallinan, S. Tsymbalov, C. R. Dorn, B. S. Pitzele and D. W. Hansen Jr, *J. Med. Chem.*, 2002, **45**, 1686.
9 G. Sandmann, C. Schneider and P. Boger, *Z. Naturforsch., C: J. Biosci.*, 1996, **51**, 534.
10 B. S. Jursic and B. W. LeBlanc, *J. Heterocycl. Chem.*, 1998, **35**, 405.
11 V. A. Ostrovskii, M. S. Pevzner, T. P. Kofman, M. B. Shcherbinin and I. V. Tselinskii, *Soc. Chim. Ital.*, 1999, 467.
12 R. N. Butler, *Comprehensive Heterocyclic Chemistry II*, ed. R. C. Storr, Pergamon, Oxford, 1996, vol. 4, pp. 621–905.
13 E. K. Harvill, R. M. Herbst, E. L. Schreiner and C. W. Roberts, *J. Org. Chem.*, 1950, **15**, 662.

14 W. G. Finnegan, R. A. Henry and R. Lofiquist, *J. Am. Chem. Soc.*, 1958, **80**, 3908.
15 Z. P. Demko and K. B. Sharpless, *J. Org. Chem.*, 2001, **66**, 7945.
16 Y. Zhou, C. Yao, R. Ni and G. Yang, *Synth. Commun.*, 2010, **1**, 2624.
17 A. Coca and E. Turek, *Tetrahedron Lett.*, 2014, **55**, 2718.
18 S. Kumar, S. Dubey, N. Saxena and S. K. Awasthi, *Tetrahedron Lett.*, 2014, **55**, 6034.
19 M. L. Kantam, K. B. S. Kumar and K. P. Raja, *J. Mol. Catal. A: Chem.*, 2006, **247**, 186.
20 V. Rama, K. Kanagaraj and K. Pitchumani, *J. Org. Chem.*, 2011, **76**, 9090.
21 G. Aridoss and K. K. Laali, *Eur. J. Org. Chem.*, 2011, 6343.
22 P. Sivaguru, K. Bhuvaneswari, R. Ramkumar and A. Lalitha, *Tetrahedron Lett.*, 2014, **55**, 5683.
23 S. Kumar, A. Kumar, A. Agarwal and S. K. Awasthi, *RSC Adv.*, 2015, **5**, 21651.
24 I. Esirden, E. Erken, M. Kaya and F. Sen, *Catal. Sci. Technol.*, 2015, **5**, 4452.
25 M. Nasrollahzadeh, Y. Bayat, D. Habibi and S. Moshaee, *Tetrahedron Lett.*, 2009, **50**, 4435.
26 B. Das, C. R. Reddy, D. N. Kumar, M. Krishnaiah and R. Narender, *Synlett*, 2010, 391.
27 Z. Du, C. Si, Y. Li, Y. Wang and J. Lu, *Int. J. Mol. Sci.*, 2012, **13**, 4696.
28 G. A. Meshram, S. Deshpande, P. A. Wagh and V. A. Vala, *Tetrahedron Lett.*, 2014, **55**, 3557.
29 F. R. Abreu, D. G. Lima, E. H. Hamu, C. Wolf and P. A. Z. Suarez, *J. Mol. Catal. A: Chem.*, 2004, **209**, 29.
30 M. Esmaeilpour, J. Javidi, F. N. Dodeji and M. M. Abarghoui, *J. Mol. Catal. A: Chem.*, 2014, **393**, 18.
31 M. Parveen, F. Ahmad, A. M. Malla and S. Azaz, *New J. Chem.*, 2015, **39**, 2028.
32 M. Nikoorazm, A. Ghorbani-Choghamarani and M. Khanmoradi, *Appl. Organomet. Chem.*, 2016, **30**, 705.
33 L. Zamania, B. B. F. Mirjalilia, K. Zomorodianb and S. Zomorodianb, *S. Afr. J. Chem.*, 2015, **68**, 133.
34 S. Bahari and A. Rezaei, *Lett. Org. Chem.*, 2014, **11**, 55.
35 F. Dehghani, A. R. Sardarian and M. Esmaeilpour, *J. Organomet. Chem.*, 2013, **743**, 87.
36 D. Habibi, M. Nasrollahzadeh, L. Mehrabi and S. Mostafaee, *Monatsh. Chem.*, 2013, **144**, 725.
37 J. Safaei-Ghomi, R. Teymuri, H. Shahbazi-Alavi and A. Ziarati, *Chin. Chem. Lett.*, 2013, **24**, 921.
38 A. Bamoniri and S. Fouladgar, *RSC Adv.*, 2015, **5**, 78483.
39 K. Kawakami and R. J. Okawara, *Organomet. Chem.*, 1966, **6**, 249.
40 B. Gutmann, J. Roduit, D. Roberge and C. O. Kappe, *Angew. Chem., Int. Ed.*, 2010, **49**, 7101.